
Temperatures in glaciers and ice sheets

Glaciers are divided into three categories, depending on their thermal structure

Cold The temperature of the ice is below the pressure melting temperature throughout the glacier, except for maybe a thin surface layer.

Temperate The whole glacier is at the pressure melting temperature, except for seasonal freezing of the surface layer.

Polythermal Some parts of the glacier are cold, some temperate. Usually the highest accumulation area, as well as the upper part of an ice column are cold, whereas the surface and the base are at melting temperature.

The knowledge of the distribution of temperature in glaciers and ice sheets is of high practical interest

- A temperature profile from a cold glacier contains information on past climate conditions.
- Ice deformation is strongly dependent on temperature (temperature dependence of the rate factor A in Glen's flow law; Appendix B).
- The routing of meltwater through a glacier is affected by ice temperature. Cold ice is essentially impermeable, except for discrete cracks and channels.
- If the temperature at the ice-bed contact is at the pressure melting temperature the glacier can slide over the base.
- Wave velocities of radio and seismic signals are temperature dependent. This affects the interpretation of ice depth soundings.

The distribution of temperature in a glacier depends on many factors. Heat sources are on the glacier surface, at the glacier base and within the body of the ice. Heat is transported through a glacier by conduction (diffusion), is advected with the moving ice, and is convected with water or air flowing through cracks and channels. Heat sources within the ice body are

- dissipative heat production (internal friction) due to ice deformation,
- frictional heating at the glacier base (basal motion)
- frictional heating of flowing water at englacial channel walls,
- release or consumption of (latent) heat due to freezing and melting.

The importance of the processes depends on the climate regime a glacier is subjected to, and also varies between different parts of the same glacier.

6.1 Energy balance equation

The energy balance equation in the form suitable to calculate ice temperature within a glacier is the advection-diffusion equation which in a spatially fixed (Eulerian) reference frame, and given by

$$\rho C \left(\underbrace{\frac{\partial T}{\partial t} + \mathbf{v} \nabla T}_{\text{advection}} \right) = \underbrace{\nabla(k \nabla T)}_{\text{diffusion}} + \underbrace{P}_{\text{production}}. \quad (6.1)$$

The ice temperature $T(\mathbf{x}, t)$ at location \mathbf{x} and time t changes due to advection, diffusion and production of heat. The material constants density ρ , specific heat capacity C and thermal conductivity k are given in Table 6.1. For constant thermal conductivity k and in one dimension (the vertical direction z and vertical velocity w) the energy balance equation (6.1) reduces to

$$\rho C \left(\frac{\partial T}{\partial t} + w \frac{dT}{dz} \right) = k \frac{d^2 T}{dz^2} + P. \quad (6.2)$$

The heat production (source term) P can be due to different processes:

Dissipation In viscous flow the *dissipation* due to ice deformation (heat release due to internal friction) is $P = \text{tr}(\dot{\boldsymbol{\epsilon}} : \boldsymbol{\sigma}) = \dot{\epsilon}_{ij} \sigma_{ji}$. Because usually the horizontal shearing deformation dominates glacier flow

$$P_{\text{def}} \simeq 2 \dot{\epsilon}_{xz} \sigma_{xz}.$$

Sliding friction The heat production is the rate of loss of potential energy as an ice column of thickness H moves down slope. If all the frictional energy is released at the bed due to sliding with basal velocity u_b ,

$$P_{\text{friction}} = \tau_b u_b \sim \rho g H \tan \beta u_b,$$

where τ_b is basal shear stress and β is the bed inclination.

Refreezing of meltwater Consider polythermal ice that contains a volume fraction μ of water. If a freezing front is moving with a velocity v_{freeze} relative to the ice, the rate of latent heat production per unit area of the freezing front is

$$P_{\text{freeze}} = v_{\text{freeze}} \mu \rho_w L.$$

Quantity	Symbol	Value	Unit
Specific heat capacity of water	C_w	4182	$\text{J K}^{-1} \text{kg}^{-1}$
Specific heat capacity of ice	C_i	2093	$\text{J K}^{-1} \text{kg}^{-1}$
Thermal conductivity of ice (at 0° C)	k	2.1	$\text{W m}^{-1} \text{K}^{-1}$
Thermal diffusivity of ice (at 0° C)	κ	$1.09 \cdot 10^{-6}$	$\text{m}^2 \text{s}^{-1}$
Latent heat of fusion (ice/water)	L	333.5	kJ kg^{-1}
Depression of melting temperature (Clausius-Clapeyron constant)			
- pure ice and air-free water	γ	0.0742	K MPa^{-1}
- pure ice and air-saturated water	γ	0.098	K MPa^{-1}

Table 6.1: *Thermal properties of ice and water.*

6.2 Steady state temperature profile

The simplest case is a vertical steady state temperature profile (Eq. 6.2 without time derivative) in stagnant ice ($w = 0$) without any heat sources ($P = 0$), and with constant thermal conductivity k . The heat flow equation (6.2) then reduces to the diffusion equation

$$\frac{d^2T}{dz^2} = 0. \quad (6.3)$$

Integration with respect to z gives

$$\frac{dT}{dz} = G \quad \implies \quad Q = k \frac{dT}{dz} = kG \quad (6.4)$$

where $G = \nabla T$ is the (constant) temperature gradient, and Q is the heat flux. Integrating again leads to

$$T(z) = Gz + T(0), \quad (6.5)$$

which means that ice temperature varies linearly with depth. Choosing for example a temperature gradient of $G = 1 \text{ K}/100 \text{ m} = 0.01 \text{ K m}^{-1} = 10 \text{ mK m}^{-1}$ gives a heat flux of $Q = kG = 0.021 \text{ W m}^{-2} = 21 \text{ mW m}^{-2}$. For comparison, typical geothermal heat fluxes are $40 - 120 \text{ mW m}^{-2}$.

To transport a geothermal heat flux of 80 mW m^{-2} through a glacier of 200 m thickness, the surface temperature has to be 8 K lower than the temperature at the glacier base.

The above calculations (partly) explain why there can be water at the base of the Greenland and Antarctic ice sheets. Under an ice cover of 3000 m and at surface temperatures of -50°C (in Antarctica), only a heat flux of $Q = k \cdot 50 \text{ K}/3000 \text{ m} = 35 \text{ mW m}^{-2}$ can be transported away. Notice that horizontal and vertical advection change this result considerably (Section 6.7).

6.3 Ice temperature close to the glacier surface

The top 15 m of a glacier are subject to seasonal variations of temperature. In this part of the glacier *heat flow (heat diffusion)* is dominant. If we neglect advection we can rewrite Equation (6.2) to obtain the well known *Fourier law* of heat diffusion

$$\frac{dT}{dt} = \kappa \frac{d^2T}{dh^2} \quad (6.6)$$

where h is depth below the surface, and $\kappa = k/(\rho C) = 1.09 \cdot 10^{-6} \text{ m}^2 \text{ s}^{-1}$ is the *thermal diffusivity* of ice. To calculate a temperature profile and changes with time we need boundary conditions. Periodically changing boundary conditions at the surface such as day/night and winter/summer can be approximated with a sine function. At depth we assume a constant temperature T_0

$$\begin{aligned} T(0, t) &= T_0 + \Delta T_0 \cdot \sin(\omega t), \\ T(\infty, t) &= T_0. \end{aligned} \quad (6.7)$$

T_0 is the mean surface temperature and ΔT_0 is the amplitude of the periodic changes of the surface temperature. The duration of a period is $2\pi/\omega$. The solution of Equation (6.6) with the boundary condition (6.7) is

$$T(h, t) = T_0 + \Delta T_0 \exp\left(-h\sqrt{\frac{\omega}{2\kappa}}\right) \sin\left(\omega t - h\sqrt{\frac{\omega}{2\kappa}}\right). \quad (6.8)$$

The solution is plotted in Figure 6.1 for realistic values of T_0 and ΔT on Colle Gnifetti (4550 m a.s.l., Monte Rosa, Valais). Notice that full ice density has been assumed for the plot, instead of a firn layer with strongly changing thermal properties, and vertical advection is neglected.

The solution (Eq. 6.8) has some noteworthy properties

- a) The amplitude varies with depth h as

$$\Delta T(h) = \Delta T_0 \exp\left(-h\sqrt{\frac{\omega}{2\kappa}}\right) \quad (6.9)$$

- b) The temperature $T(h, t)$ has an extremum when

$$\sin\left(\omega t - h\sqrt{\frac{\omega}{2\kappa}}\right) = \pm 1 \quad \Rightarrow \quad \omega t - h\sqrt{\frac{\omega}{2\kappa}} = \frac{\pi}{2}$$

and therefore

$$t_{\max} = \frac{1}{\omega} \left(\frac{\pi}{2} + h\sqrt{\frac{\omega}{2\kappa}} \right) \quad (6.10)$$

The phase shift is increasing with depth below the surface.

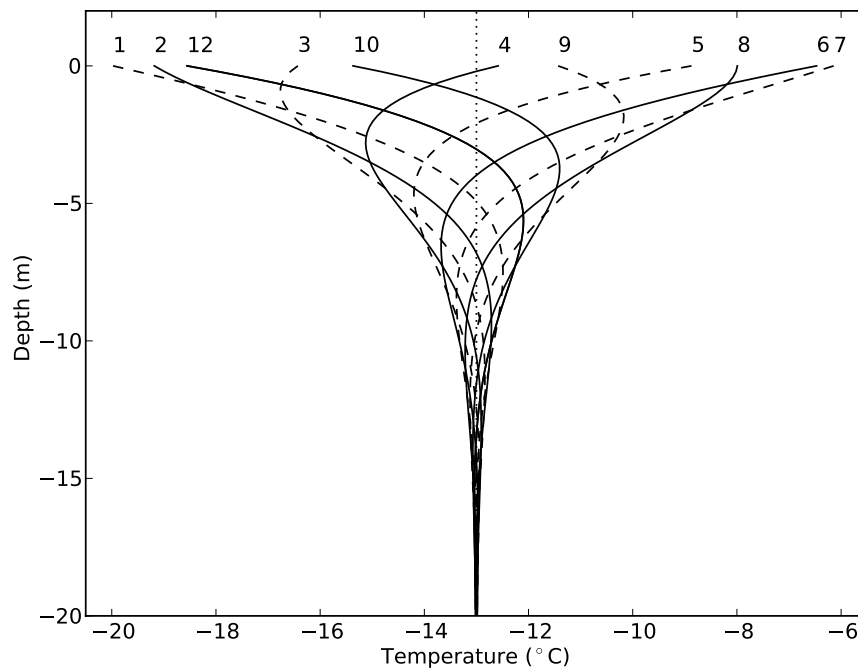


Figure 6.1: Variation of temperature with depth for the conditions at Colle Gnifetti. Numbers next to curves indicate months (1 corresponds to January).

c) The heat flux $Q(h, t)$ in a certain depth h below the surface is

$$Q(h, t) = -k \frac{\partial T}{\partial h} = (\text{complicated formula that is easy to derive})$$

For the heat flux $Q(0, t)$ at the glacier surface we get

$$Q(0, t) = \Delta T_0 \sqrt{\omega \rho C k} \sin\left(\omega t + \frac{\pi}{4}\right)$$

$Q(0, t)$ is maximal when

$$\sin\left(\omega t + \frac{\pi}{4}\right) = 1 \quad \Rightarrow \quad \omega t + \frac{\pi}{4} = \frac{\pi}{2} \quad \Rightarrow \quad t_{\max} = \frac{\pi}{4\omega}$$

where t_{\max} is the time when the heat flux at the glacier surface is maximum.

$$\text{Temperature:} \quad t_{\max} = \frac{\pi}{2\omega}$$

$$\text{Heat flux:} \quad t_{\max} = \frac{\pi}{4\omega}$$

The difference is $\pi/(4\omega)$ and thus 1/8 of the period. The maximum heat flux at the glacier surface is 1/8 of the period ahead of the maximum temperature. For a yearly cycle this corresponds to 1.5 months.

- d) From the ratio between the amplitudes in two different depths the heat diffusivity κ can be calculated

$$\frac{\Delta T_2}{\Delta T_1} = \exp\left((h_1 - h_2)\sqrt{\frac{\omega}{2\kappa}}\right) \quad \Longrightarrow \quad \kappa = \frac{\omega}{2} \left(\frac{h_2 - h_1}{\ln \frac{\Delta T_2}{\Delta T_1}}\right)^2$$

There are, however, some restrictions to the idealized picture given above

- The surface layers are often not homogeneous. In the accumulation area density is increasing with depth. Conductivity k and diffusivity κ are functions of density (and also of temperature).
- In nature the surface boundary condition is not a perfect sine function.
- The ice is moving. Heat diffusion is only one part, heat advection may be equally important.
- Percolating and refreezing melt water can drastically change the picture by providing a source of latent heat (see below).

Superimposed on the yearly cycle are long term temperature changes at the glacier surface. These penetrate much deeper into the ice, as can be seen from Equation (6.9), since ω decreases for increasing forcing periods.

In spring or in high accumulation areas the surface layer of a glacier consists of snow or firn. If surface melting takes place, the water percolates into the snow or firn pack and freezes when it reaches a cold layer. The freezing of 1 g of water releases sufficient heat to raise the temperature of 160 g of snow by 1 K. This process is important to “annihilate” the winter cold from the snow or firn cover in spring, and is the most important process altering the thermal structure of high accumulation areas and of the polar ice sheets.

6.4 Temperate glaciers

In a temperate glacier, all heat that is produced at the boundaries or within the glacier is used to melt ice. This means that temperate glaciers contain liquid water that is stored in cracks and voids, and also within the ice matrix. The water content μ of temperate ice is small, usually between 0.1 and 4 volume percent. The water is stored in veins and triple junctions between the ice grains, where it can slowly percolate through the ice matrix if veins are not blocked by air bubbles. The water between ice grains has an important effect on the deformation properties of ice, and it affects the rate factor A in Glen’s flow law (Duval, 1977; Paterson, 1999)

$$\begin{aligned} A(\mu) &= (3.2 + 5.8\mu) \cdot 10^{-15} \text{ kPa}^{-3} \text{ s}^{-1} \\ &= (101 + 183\mu) \text{ MPa}^{-3} \text{ a}^{-1}, \end{aligned} \quad (6.11)$$

where μ is the percentage of water within the ice.

Pressure melting point temperature

For pure ice the melting temperature T_m depends on absolute pressure p by

$$T_m = T_{tp} - \gamma(p - p_{tp}), \quad (6.12)$$

where $T_{tp} = 273.16 \text{ K}$ and $p_{tp} = 611.73 \text{ Pa}$ are the triple point temperature and pressure of water. The Clausius-Clapeyron constant is $\gamma_p = 7.42 \cdot 10^{-5} \text{ K kPa}^{-1}$ for pure water/ice. Since glacier ice contains soluble and insoluble chemicals and air bubbles, the value of γ can be as high as $\gamma_a = 9.8 \cdot 10^{-5} \text{ K kPa}^{-1}$ for air saturated water (Harrison, 1975).

6.5 Cold glaciers

In cold glaciers heat flow is driven by temperature gradients. Usually the base is warmest due to dissipation, friction and geothermal heat. This has the consequence that heat is flowing from the base into the ice body, warming up the ice. Advection of warm or cold ice strongly influences local ice temperature.

Only the highest glaciers in the Alps are completely cold, with a lower limit of about 3900 m a.s.l.. The most famous of these is Colle Gnifetti (4550 m a.s.l.), the highest accumulation basin of the Gorner-/Grenzletscher system. At temperatures of about -13° C the ice conserves atmospheric conditions such as impurities and air bubbles. Surface melting only takes place on exceptionally hot days and leads to formation of ice lenses. Many ice cores have been drilled on Colle Gnifetti and were investigated in the laboratory to obtain the climate history of central Europe.

Figure 6.2 shows two temperature profiles measured in boreholes 200 m apart on the same flow line on Colle Gnifetti. In the absence of advection and density gradients one would expect straight steady state temperature profiles (cf. Eq. 6.5). The unequal curvature of the modeled steady state profiles (blue and red curve in Fig. 6.2a) is due to firn density and different advection regimes. This shows that the interpretation of temperature profiles to deduce past climate can be quite tricky.

The marked bend towards warmer temperature at 30 m depth is due to changing surface temperatures. Numerical modeling showed that the temperature increase by 1° C around 1990 is mainly responsible for this feature (the profiles were measured in 1995/96; in 1982 the transient profiles looked like the steady state configuration).

Modeling the advection and conduction of heat in a glacier is usually not sufficient. The geothermal heat flux close to the glacier base is affected by the ice temperature, and therefore by the glacier flow, and the flux of meltwater. At Colle Gnifetti the measured (and modeled) temperature gradients at the glacier base are different due

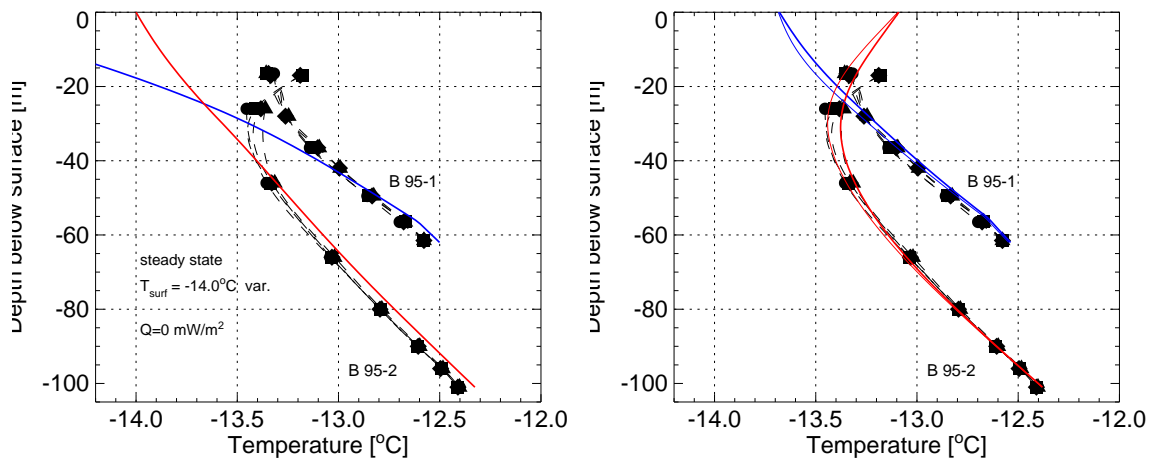


Figure 6.2: Markers indicate temperatures measured in two boreholes on the same flow line, 200 m apart, on Colle Gnifetti. Solid lines are the results of numerical interpretation of the data with steady state (left) and transient (right) temperature evolution. Notice that the different curvature of the steady state profiles is due to firn density and advection. From Lüthi and Funk (2001).

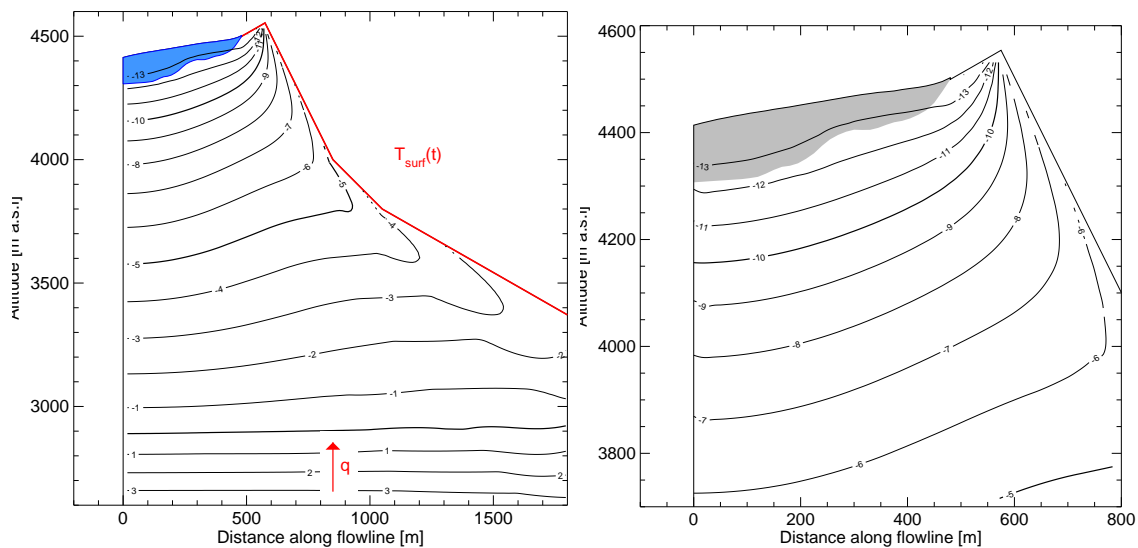


Figure 6.3: Modeled temperature distribution within the Monte Rosa massif. Notice the highly increased surface temperature on the south (right) face which leads to horizontal heat fluxes close to steep mountain faces. Thawing permafrost at the base of the mountain was essential to reproduce the measured heat flux at the glacier base. From Lüthi and Funk (2001).

to different distance to the south-facing rock wall of Monte Rosa. Figure 6.3 shows the temperature distribution in the whole massif, with the glacier on top. Notice that there are areas within the mountain where heat flows horizontally (heat always flows perpendicular to the isotherms). Heat flux at sea level was assumed to be 70 mW m^{-2} , but it had to be greatly reduced to match the observed fluxes. In the model this was accomplished with freezing/thawing ice within the rock (permafrost), which is a reaction to climate changes since the last ice age. The lowest calculated permafrost margin was at about 2900 m elevation.

6.6 Polythermal glaciers and ice sheets

Polythermal glaciers are usually cold in their core and temperate close to the surface and at the bed. Heat sources at the surface are from the air (sensible heat flux), direct solar radiation (short wave), thermal radiation (long wave), and the penetration and refreezing of melt water (convection and latent heat). The temperate layer at the bed can be of considerable thickness and is caused by geothermal heat flux and heat dissipation due to friction and ice deformation. The latter is highest close to the base because stresses and strain rates are highest there.

Gorner-/Grenzgletscher is the biggest polythermal glacier in the Alps. Cold ice originating from Colle Gnifetti (4500 m a.s.l.) is advected down to the confluence area at 2500 m a.s.l., and all the way to the glacier tongue. Figure ?? shows the slow cooling of a borehole in the confluence area after hot-water drilling. After equilibration, a cold central core is apparent in Figure 6.4 which was advected from the high accumulation area, and is gradually warming along the flow line (Figure 6.5, mostly due to heat conduction. The cold ice is mostly impermeable to water which leads to the formation of deeply incised river systems and surficial lakes which sometimes drain through crevasses or *moulins*.

Nice examples of the polythermal structure of the Greenland ice sheet are the temperature profiles in Figure 6.6, measured in Jakobshavn Isbræ, Greenland (Iken et al., 1993; Funk et al., 1994; Lüthi et al., 2002). The drill sites are located 50 km inland of the margin of the Greenland ice sheet, at a surface elevation is 1100 m a.s.l., where ice thickness on the ice sheet is 830 m, but about 2500 m in the ice stream center.

In Figure 6.6 (bottom left) temperatures are highest close to the surface and close to the bed. The thick, very cold layer in between is advected from the inland parts of the ice sheet (see Figure 6.7 top). The lowest 31 m are at the pressure melting temperature $T_m = -0.55^\circ \text{C}$. A quick calculation with Equation (6.12) and

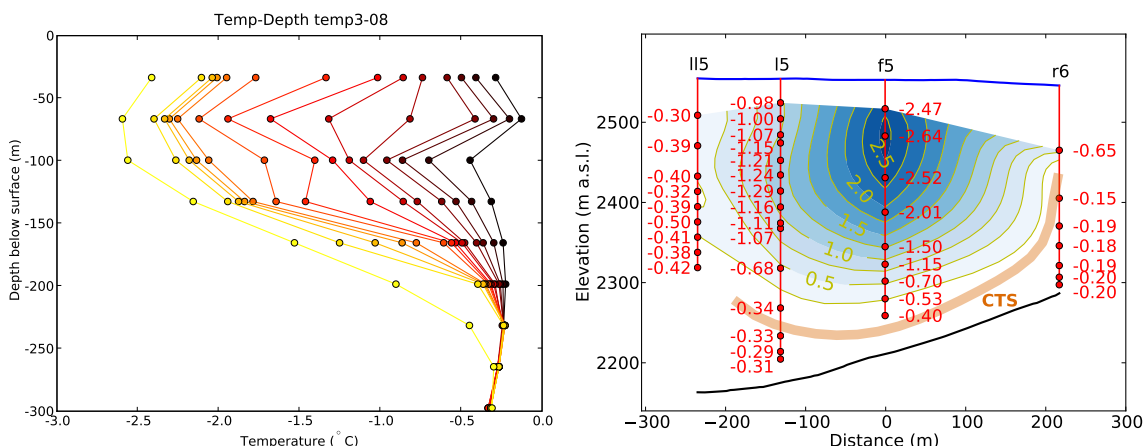


Figure 6.4: *Left: Cooling of a borehole drilled in the confluence area of Gorner-/Grenzgletscher. Temperatures measured every day after completion of drilling are shown in increasingly lighter colors, and after three months (leftmost yellow curve) (from Ryser, 2009). Right: Cross section through the glacier showing an onion-like structure of ice temperature, due to advection of cold ice (from Ryser et al., 2013).*

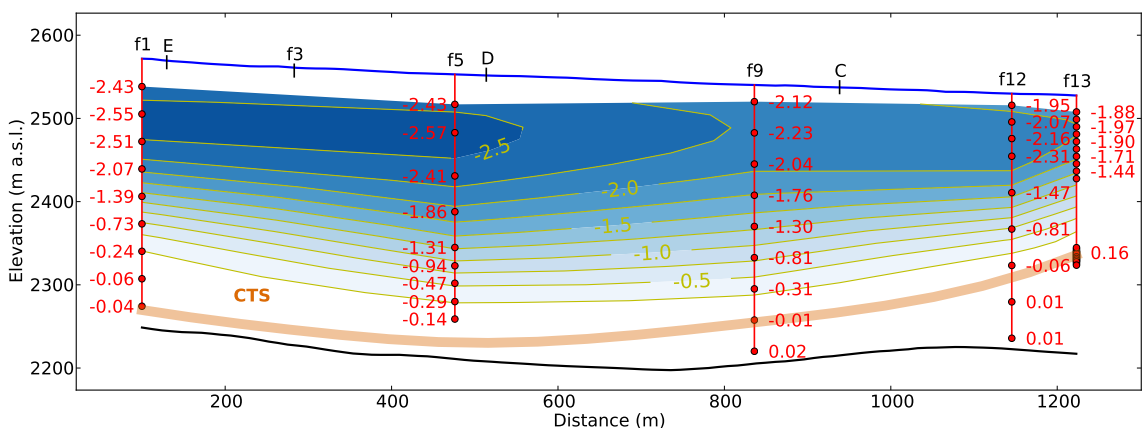


Figure 6.5: *Longitudinal section through the glacier showing the advection of cold ice which is gradually warming due to heat flow on its way towards the terminus (from Ryser et al., 2013).*

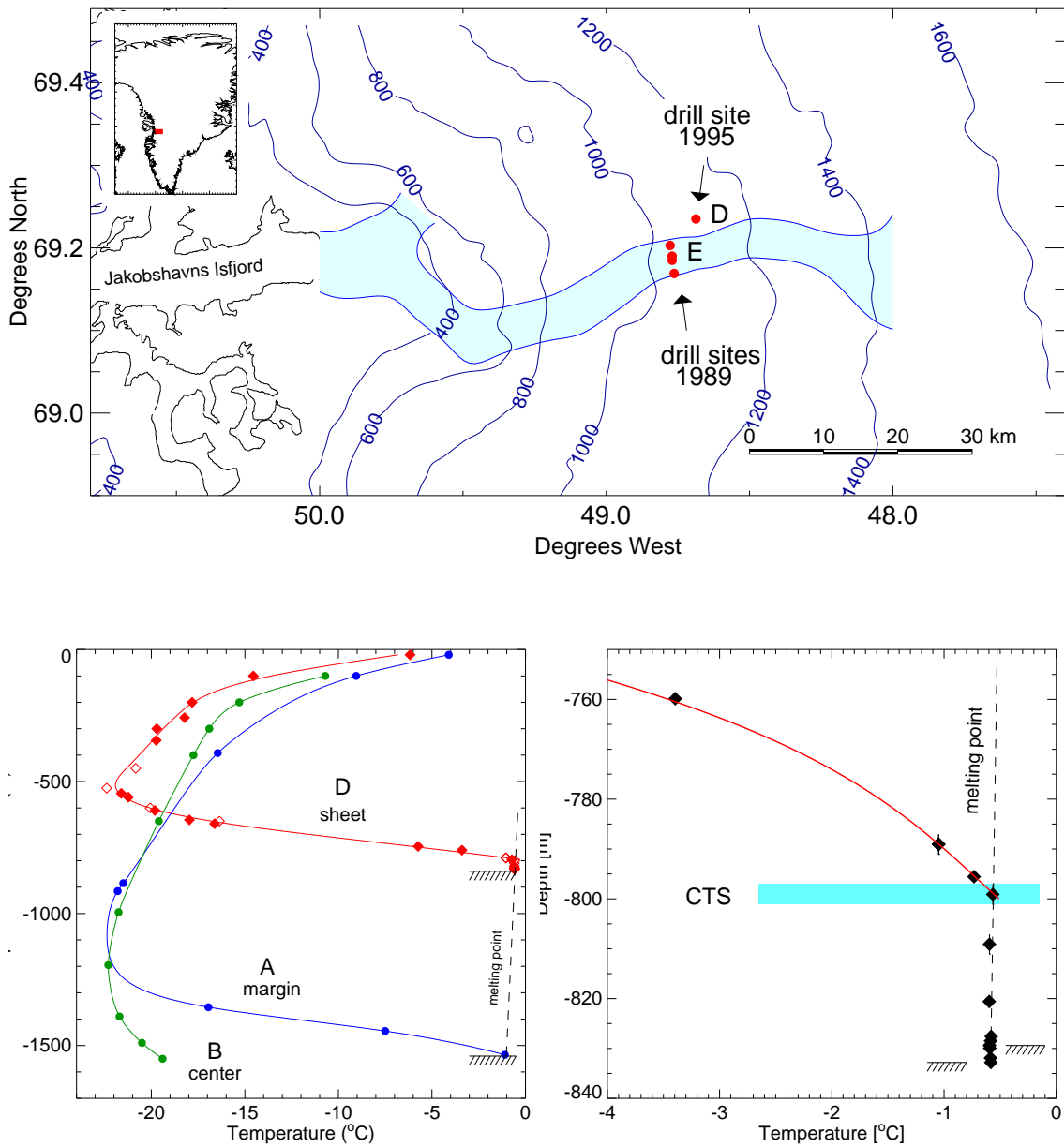


Figure 6.6: *Top: Location map of the drill sites on Jakobshavn Isbræ, Greenland, where temperature profiles have been measured. Left: Profile A is from the southern side of the ice stream, profile B from the center (the ice is about 2500 m thick there) and D on the northern margin. Notice the basal temperate ice at D and also at A. The very cold ice in the middle of the profiles is advected and is slowly warming up. Right: Closeup of the 31 m thick temperate layer at site D. The cold-temperate transition surface CTS is at freezing conditions. The Clausius-Clapeyron gradient (dashed line) is $\gamma = 0.0743 \text{ K MPa}^{-1}$. From Lüthi et al. (2002).*

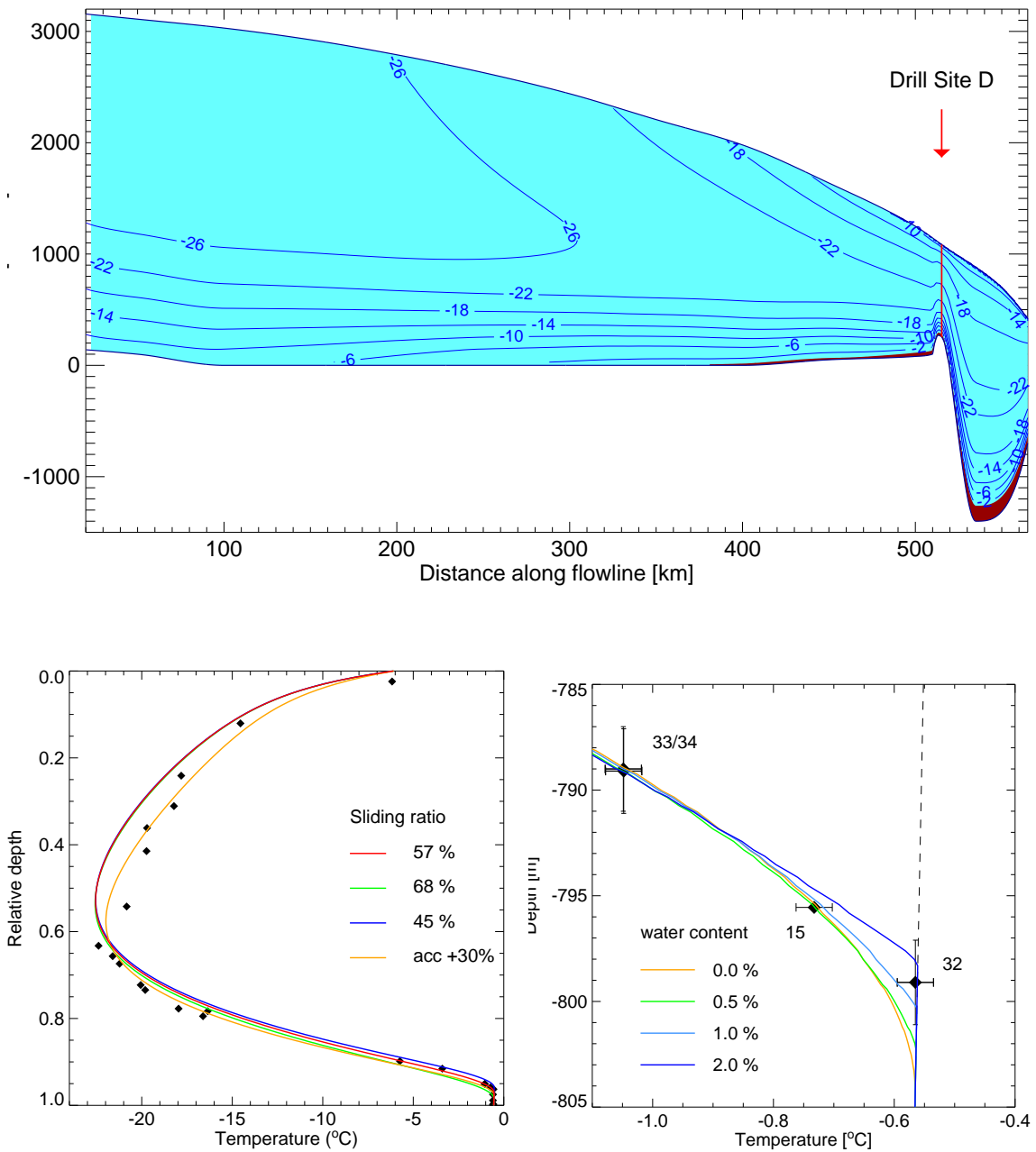


Figure 6.7: *Top: Temperature distribution along a flow line in the Greenland Ice Sheet, and passing through drill site D. Clearly visible is the advection of cold ice and the onset of a basal temperate layer far inland at 380 km. Left: Modeled temperature profiles for different ratios of basal motion. Right: Modeled temperature profiles for different values of the water content in the temperate ice. From Funk et al. (1994) and Lüthi et al. (2002).*

reasonable values for the ice density and gravity gives

$$\begin{aligned} T_m &= T_{tp} - \gamma_p(p - p_{tp}) = T_p - \gamma_p(\rho g H - p_{tp}) \\ &= 273.16 \text{ K} - 7.42 \cdot 10^{-5} \text{ K kPa}^{-1} (900 \text{ kg m}^{-3} \cdot 9.825 \text{ m s}^{-2} \cdot 830 \text{ m}) \\ &\simeq 273.16 \text{ K} - 0.545 \text{ K} \simeq 272.615 \text{ K} = -0.54^\circ \text{ C}. \end{aligned} \quad (6.13)$$

The strong curvature of the temperature profiles where they are coldest indicates that the ice is warming (explain why!). Upward heat flux from the temperate zone close to the base is very high. The temperature gradient just above the CTS (800 m depth) in profile D is 0.048 K m^{-1} . The upward heat flux therefore is (per unit area)

$$Q = k \frac{dT}{dz} \simeq 2.1 \text{ W m}^{-1} \text{ K}^{-1} \cdot 0.048 \text{ K m}^{-1} \simeq 0.1 \text{ W m}^{-2}. \quad (6.14)$$

This heat has to be produced locally, since heat fluxes in the temperate zone below 800 m depth are downward (away from the CTS), but very small due to the Clausius-Clapeyron temperature gradient. The only way to produce this heat is by freezing the water contained within the temperate ice. From a flow model we know that the CTS moves with respect to the ice by $v_{\text{freeze}} \sim 1 \text{ m a}^{-1}$. With a moisture content of $\mu = 1\%$ (by volume) we obtain a heat production rate of

$$\begin{aligned} P &= \mu v_{\text{freeze}} \rho_w L \simeq 0.01 \cdot 1 \text{ m a}^{-1} \cdot 1000 \text{ kg m}^3 \cdot 3.33 \cdot 10^5 \text{ J kg}^{-1} \\ &= 3.55 \text{ MJ a}^{-1} \text{ m}^{-3} \simeq 0.113 \text{ W m}^{-3} \end{aligned} \quad (6.15)$$

which matches up nicely with the heat transported away by diffusion (Eq. 6.14). A detailed analysis with the flow model shows that the most likely value for the water content is about 1.5% (Fig. 6.7, bottom right). Another interesting result from the model is that an ice column passing through drill site D has already lost the lowest 40 m through melting at the glacier base.

6.7 Advection – diffusion

Close to the ice divides in the central parts of an ice sheet, the ice velocity is mainly vertical down. Under the assumptions of only vertical advection, no heat generation, and a frozen base we can calculate the steady state temperature profile with the simplified Equation (6.2)

$$\kappa \frac{d^2 T}{dz^2} = w(z) \frac{dT}{dz} \quad (6.16)$$

The boundary conditions are

$$\begin{array}{ll} \text{surface:} & z = H : \quad \text{temperature } T_s = \text{const} \\ \text{bedrock:} & z = 0 : \quad \text{heat flux } -k \left(\frac{dT}{dz} \right)_B = G = \text{const} \end{array}$$

For the first integration we substitute $f = \frac{dT}{dz}$ so that $\kappa f' = wf \implies \frac{f'}{f} = \frac{1}{\kappa}w$ with the solution

$$\frac{dT(z)}{dz} = \left(\frac{dT}{dz} \right)_B \exp \left(\frac{1}{\kappa} \int_0^z w(z) dz \right). \quad (6.17)$$

Now we make the assumption that the vertical velocity is $w(z) = w_s z/H$, with the vertical velocity at the surface equal to the net mass balance rate $w_s = -\dot{b}$. With the definition $l^2 := 2\kappa H/\dot{b}$ we get

$$T(z) - T(0) = \left(\frac{dT}{dz} \right)_B \int_0^z \exp \left(-\frac{z^2}{l^2} \right) dz \quad (6.18)$$

which has the solution

$$T(z) - T_s = \frac{\sqrt{\pi}}{2} l \left(\frac{dT}{dz} \right)_B \left[\operatorname{erf} \left(\frac{z}{l} \right) - \operatorname{erf} \left(\frac{H}{l} \right) \right]. \quad (6.19)$$

The so-called *error function* is tabulated and implemented in all mathematical softwares (usually as `erf`), and is defined as

$$\operatorname{erf}(x) = \frac{2}{\sqrt{\pi}} \int_0^x \exp(-x^2) dx.$$

We now introduce the useful definition of the *Péclet Number* $Pe = w_s H/\kappa$ which is a measure of the relative importance of advection and diffusion. The shape of the temperature profiles in Figure 6.8 only depends on the Péclet Number. Depth and temperature can be scaled by the dimensionless variables

$$\begin{aligned} \text{scaled distance above bed} & \quad \xi = \frac{z}{H}, \\ \text{scaled temperature} & \quad \Theta = \frac{k(T - T_s)}{GH}. \end{aligned}$$

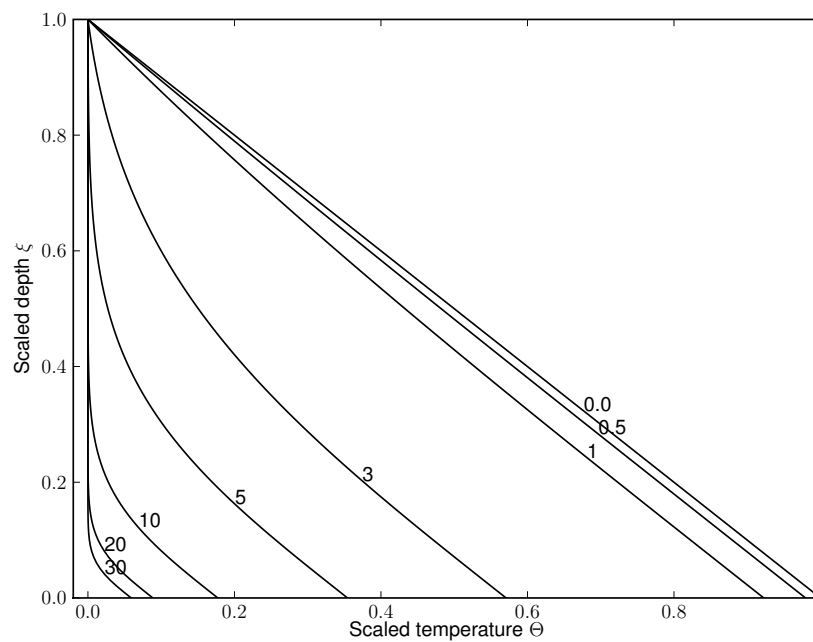


Figure 6.8: *Dimensionless steady temperature profiles in terms of the dimensionless variables ξ and Θ for various values of the Péclet number Pe (next to curves). At high Péclet numbers the advection dominates, and cold ice is transported down from the surface into vicinity of the bed.*

